Polyhedron 161 (2019) 213–221

Contents lists available at ScienceDirect

Polyhedron

journal homepage: www.elsevier.com/locate/poly

Cobalt and copper complexes with formamidine ligands: Synthesis, crystal X-ray study, DFT calculations and cytotoxicity

Ahmed A. Soliman [a,*], Mina A. Amin [a,*], Amany M. Sayed [b], Azza A.A. Abou-Hussein [c], Wolfgang Linert [d]

[a] Department of Chemistry, Faculty of Science, Cairo University, 12613 Giza, Egypt
[b] Hazard Waste Management Division, Ministry of Environmental Affairs, Cairo, Egypt
[c] Faculty of Women for Arts, Science and Education, Ain Shams University, Heliopolis, Cairo, Egypt
[d] Institute of Applied Synthetic Chemistry, Vienna University of Technology, Getreidemarkt, 9163-AC, A-1060 Vienna, Austria

ARTICLE INFO

Article history:
Received 11 September 2018
Accepted 4 December 2018
Available online 20 December 2018

Keywords:
Copper
Cobalt
Formamidine
X-ray
Cytotoxicity

ABSTRACT

Co(II) and Cu(II) complexes with distorted octahedral and distorted square planar geometries of the type $[Co(L_2)_2(H_2O)_2](NO_3)_2$ and $[Cu(L_1)_2Cl_2]$ have been prepared and characterized using elemental analysis, IR and crystal X-ray studies. The two complexes were prepared with two novel formamidine ligands, N′-(benzothiazol-2-yl)-N,N-dimethylformamidine (L_1) and N-(pyridin-2-yl)formamidine (L_2). $[Cu(L_1)_2Cl_2]$ crystallized in the space group $P2_1/c$, $a = 8.5987(3)$ Å, $b = 15.9778(6)$ Å, $c = 10.6308(7)$ Å, $V = 1321.07(11)$ Å^3, $Z = 4$. $[Co(L_2)_2(H_2O)_2](NO_3)_2$ crystallized in the space group $P21/c$, $a = 7.9187(2)$ Å, $b = 10.8117(4)$ Å, $c = 11.6687(5)$ Å, $V = 902.13(6)$ Å^3, $Z = 4$. The existence of H-bonding in the complex $[Co(L_2)_2(H_2O)_2](NO_3)_2$ is discussed. The negative values of the electronic energies (−2329.59 to −4461.21 a.u.), the highest occupied molecular orbital energies (−0.2311 to −0.2590 a.u.) and the lowest unoccupied molecular orbital energies (−0.063 to −0.08525 a.u.) of the complexes indicate the stability of the complexes. The complexes have noticeable cytotoxicity with IC_{50} (μmole/well) values of 0.002 and 0.047 (MCF-7), 0.0048 and 0.051 (HCT-116), 0.0014 and 0.044 (HepG-2) for the copper and cobalt complexes; respectively.

1. Introduction

Transition metal complexes with heterocyclic compounds containing nitrogen and sulfur atoms are of great importance in many areas, such as medicinal chemistry, material science, catalysis, photochemical activation of CO_2 and magnetism [1–11]. Since the discovery of the antitumor activity of cisplatin [12,13], many attempts have been carried out to design other inexpensive transition metal complexes, like copper and cobalt complexes, with different ligands [14]. Both Cu and Co can form a wide range of complex geometries due to their stereochemical flexibility that allows them to coordinate N-based heterocyclic compounds, which play an important role in many biological systems [15]. Formamidine derivatives and their related compounds have been extensively used as biologically active complexing and analytical reagents [16–20]. Due to the feasibility of the synthesis of formamidine ligands, different studies involve the development of formamidine based ligands to get more biologically active ligands. Ligands with different coordinating atoms (N and S) can interact with soft and hard Lewis acid metal centers through either the N or S atoms, or both, giving dimers, linkage isomers or polymeric structures.

Co(II) metal is essential for human metabolism and it plays a vital role (within vitamin B12) in DNA synthesis. Co(II) complexes also exhibit biological activities, like antitumor activity for leukemia and lymphoma cell lines [21] and antimicrobial activity [22]. Density Functional theory (DFT) has been used to study the electronic structures together with the vibrational and absorption spectra of metallic complexes [23–27].

Cu(II) metal exists in enzymes in biological systems [28] and its metal complexes exhibit several biological activities, like antineoplastic activity [29] and antifungal/antibacterial [30] and antitumor activities [31]. Cu(II) metal complexes with N, O and S donor based ligands show good antitumor activities due to their strong binding abilities with the DNA base pair [32,33]. The Cu(II) ion acts as an intermediate Lewis acid and it can interacts with N and S atoms with a higher tendency towards the nitrogen atom [34–37] and is expected to form metal complexes with the formamidine ligand.

* Corresponding authors. Fax: +20 235727556 (A.A. Soliman).
E-mail addresses: asoliman@sci.cu.edu.eg (A.A. Soliman), maa580@york.ac.uk (M.A. Amin).

https://doi.org/10.1016/j.poly.2018.12.020
0277-5387/

In continuation of our previous studies on formamidine ligands [38–40], we report here the structures of trans cobalt and copper complexes with two different formamidine ligands. DFT calculations were performed in order to highlight the relationship between the structures and electronic properties of the complexes. The structures of the formamidine ligands are given in Scheme 1.

2. Experimental

2.1. Materials and physical measurements

All the chemicals used in this study were of the highest purity available. The infrared spectra of the compounds were recorded using a Jasco FT-IR – 460 plus (range 400–4000 cm^{-1}). UV–Vis spectra were recorded using an Optizen UV–Vis spectrophotometer with a 1 cm path length quartz cell. ^1H NMR spectra were recorded in DMSO-d_6 using a Varian-Oxford Mercury VX-300 NMR (300 MHz) spectrometer.

2.2. X-ray crystal structure determination of the complexes

The crystals were obtained by recrystallization of the complexes from ethanol by slow evaporation. The crystal data were collected on a Nonius Kappa-CCD area detector diffractometer [41] equipped with graphite monochromated Mo Ka radiation (λ = 0.71073 Å). All calculations were performed using the MAXUS crystallographic software package (Bruker Nonius, Delft & MacScience, Japan). The structures of the Cu(II) and Co(II) complexes were solved by the direct method and refined by the full-matrix least-squares method on F^2. The non-hydrogen atoms have been refined anisotropically. The H-atoms were placed in calculated positions and refined isotropically with a riding model. Atomic scattering factors were taken from the International Tables for Crystallography [42]. Molecular graphics for the complexes are from ORTEP [43]. A summary of the crystal data and refinement results of $[Cu(L_1)_2Cl_2]$ and $[Co(L_2)(H_2O)_2](NO_3)_2$ is listed in Table 1. The molecular structures and crystal packing diagrams are given in Figs. 1–4.

2.3. DFT calculations

The molecular structures of the complexes in the ground state were computed with DFT using the UB3LYP correlation functional [44,45] in addition to the 6-31G(d+) basis set [46,47] using GAUSSIAN 09 [48] in the gas phase and the output files were viewed by the GaussView 05 program. The X-ray structural data of the complexes were used to generate the initial structures of the prepared complexes. The optimized complexes were subjected to a frequency calculation at the DFT level. The electronic spectra of the ligands and complexes were calculated with the TD-DFT method. The optimized geometries of the prepared complexes and ligands are shown in Figs. S1–S4. Selected bond angles, bond lengths and atomic charges of the compounds are listed in Tables S12 and S2. The infrared vibrational band assignments of the ligands and complexes have been made using the GaussView molecular visualization software.

2.4. Evaluation of the antitumor activity

The cytotoxicity testing was carried out using a rapid colorimetric assay for cellular growth and survival [49]. The human breast cancer cell line (MCF-7 cells), human colon carcinoma cell line (HCT-116 cells), human hepatocellular cancer cell line (HepG-2 cells), HEP-2 (larynx carcinoma cells) and HELA (cervical carcinoma cells) were used as cell lines to test for the cytotoxicity of the complexes under study. All cell lines were obtained from the Tissue Culture Unit (Vacsera). The tumor cells were cultured in Dulbecco's modified Eagle's medium (DMEM) or RPMI-1640, depending on the type of cell line, supplemented with 10% heat-inactivated fetal bovine serum, 1% L-glutamine, HEPES buffer and 50 μg/ml gentamycin. The cells were incubated at 37 °C in a humidified atmosphere with 5% CO_2 and were sub cultured two times a week during the experimentation. The cytotoxicity experiments were repeated three times to get the best statistical results. The experiments were carried out in the Tissue Culture Unit at the Regional Centre for Mycology and Biotechnology RCMB, Al-Azhar University, Cairo, Egypt.

2.5. Synthesis of the formamidine ligands

A mixture of dimethoxy-N-dimethylmethanamine (0.238 g, 2.0 mmol) and either of benzothiazole-2-amine (L_1) or pyridine-2-amine (L_2) (0.188 g, 2 mmol) were mixed together in toluene and heated to reflux for 8 hours (Schemes 2 and 3) [50]. The color of the reaction mixture changed from transparent to white, and a precipitate was formed. The reaction mixture was cooled and the solvent was rotatory evaporated. The isolated white ligand was washed several times with methyl alcohol. The ligand was left to dry at room temperature under a vacuum. The isolated precipitate was found to be soluble in most common solvents (ethyl alcohol, benzene, toluene, tetrahydrofurane, dioxane, hexane and dimethylformamide). It is worth mentioning that L_2 is formed with the removal of the dimethyl groups; Scheme 1.

L_1: *Anal.* Calc. for $C_{10}H_{11}N_3S$ (205.28), Calc.: C, 58.51; H, 5.40; N, 20.47; Found: C, 58.32; H, 5.28; N, 20.18 %. IR (KBr, cm^{-1}): 3018–2920 ν(C—H), 1620 ν(C=N), 1242 ν(C—N). ^1H NMR (δ, ppm): 8.37 s (1H; CH aldimine), 7.17–7.71 m (4H; Ph), 3.08–3.13 m (6H; $2CH_3$).

L_2: *Anal.* Calc. for $C_6H_7N_3$ (121.19), Calc.: C, 59.41; H, 5.82; N, 34.66; Found: C, 59.32; H, 5.74; N, 34.70%. IR (KBr, cm^{-1}): 3043–2916 ν(C—H), 1631 ν(C=N), 1265 ν(C—N). ^1H NMR (δ, ppm): 8.07 s (1H; CH aldimine), 6.49–7.19 m (4H; 4CH pyridine), 2.62–2.67 m (6H; $2CH_3$).

2.6. Synthesis of the $[Cu(L_1)_2Cl_2]$ and $[Co(L_2)_2(H_2O)_2](NO_3)_2$ complexes

The ligand L_1 (0.21 g, 1.0 mmol) was dissolved in 10 mL of ethanol and gradually added to $CuCl_2{\cdot}H_2O$ (0.17 g, 1.0 mmol), also dissolved in 10 mL of ethanol. The mixture was left in a refrigerator

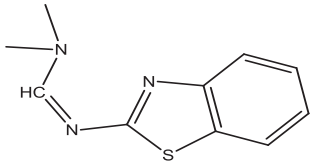

(Z)-N'-(benzo[d]thiazol-2-yl)-N,N-dimethylformamidine (**L_1**)

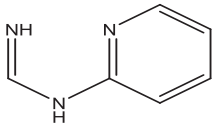

N-(pyridin-2-yl)formamidine (**L_2**)

Scheme 1. The formamidine ligands.

Table 1
X-ray structural data.

Compound	HOMO	LUMO	χ	η	σ	Pi	ΔE	ω	ΔN_{max}
L_1	−0.20	−0.048	0.127	0.079	12.64	−0.127	0.158	0.103	1.61
L_2	−0.22	−0.028	0.125	0.097	10.31	−0.125	0.194	0.081	1.29
$[Cu(L_1)_2Cl_2]$	−0.23	−0.063	0.146	0.083	11.97	−0.146	0.167	0.128	1.75
$[Co(L_2)(H_2O)_2](NO_3)_2$	−0.25	−0.085	0.167	0.082	12.12	−0.167	0.165	0.170	2.03

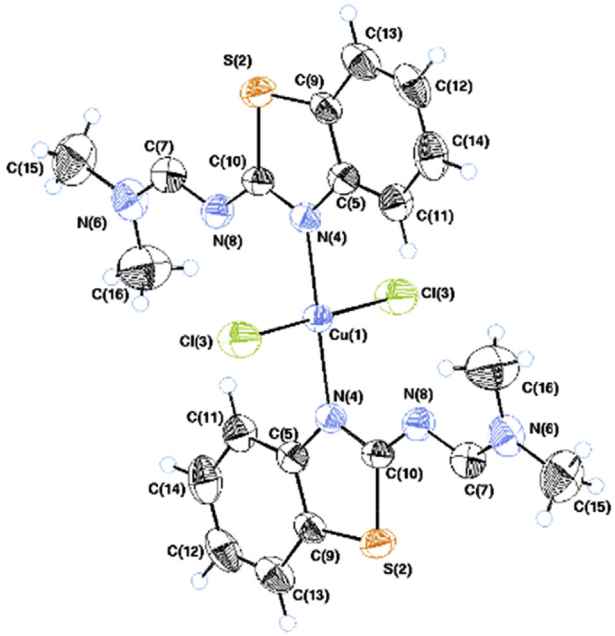

Fig. 1. ORTEP diagram of $[Cu(L_1)_2Cl_2]$.

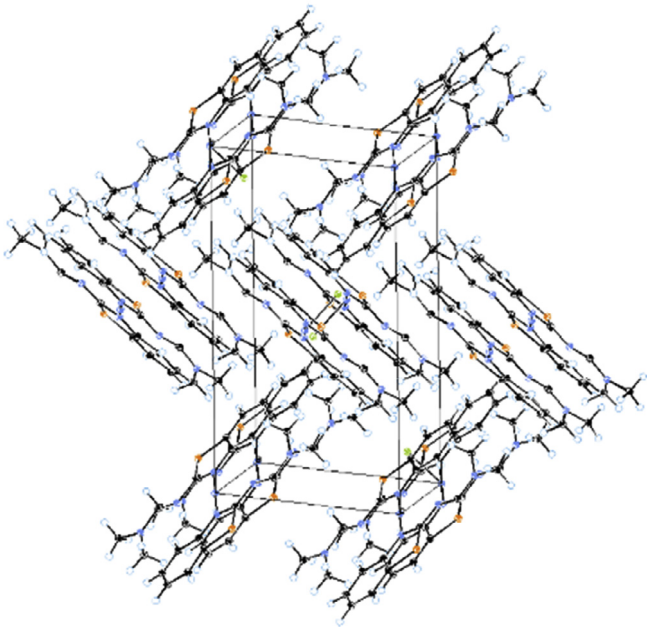

Fig. 2. Packing of $[Cu(L_1)_2Cl_2]$.

for several weeks, after which monoclinic blue crystals of $[Cu(L_1)_2Cl_2]$ separated out. The $[Co(L_2)(H_2O)_2](NO_3)_2$ complex was prepared in a similar way, mixing ligand L_2 (0.12 g, 1.0 mmol) with $Co(NO_3)_2{\cdot}6H_2O$ (0.29 g, 1.0 mmol). The complexes were filtered off and dried.

$[Cu(L_1)_2Cl_2]$: *Anal.* Calc. for $C_{10}H_{11}Cl_2N_3SCu$, Calc.: C, 35.32; H, 3.24; N, 12.36; Found: C, 35.54; H, 3.21; N, 12.14%. IR (KBr, cm^{-1}): 1636 ν(C═N), 1292 ν(C═N), 427 ν(Cu—Cl), 361 ν(Cu—N).

$[Co(L_2)_2(H_2O)_2](NO_3)_2$: *Anal.* Calc. for $C_6H_{11}N_5O_8Co$, Calc.: C, 21.17; H, 3.23; N, 20.58, Found: C, 21.01; H, 3.14; N, 20.64%. IR (KBr, cm^{-1}): 1655 ν(C═N), 1277 ν(C═N), 536 ν(Co—O), 434 ν(Co—N).

3. Results and discussion

3.1. Spectroscopic data

The IR spectra of the Co(II) and Cu(II) complexes were compared with those of the free ligands in order to investigate any change in the vibration frequencies upon coordination with the metal centers. All the characteristic peaks of the ligands and the complexes are given in Table S3. The IR spectrum of N′-(benzothiazol-2-yl)-N,N-dimethylformamidine (L_1) (Fig. S5) shows a characteristic band at 1279 cm^{-1} which is assigned to the stretching vibration of the C—N group. A strong band appears at 1619 cm^{-1}, which could be due to the stretching frequency of the (C═N) group. These C—N and C═N stretching bands remain in the spectrum of the complex but are shifted to 1292 and 1636 cm^{-1}; respectively [51], indicating the involvement of these groups in coordination with the Cu(II) ion. The Cu(II) complex also shows also a characteristic peak at 512 cm^{-1}, which is assigned to the Cu—N bond [52]. This coordination mode was also confirmed by the X-ray crystal structure. The theoretical vibrational spectrum of the copper complex is in good agreement with the experimental one, as shown in Figs. S5 and S6. The calculated C═N strong absorptions occurs at 1672 cm^{-1} for the copper complex and this value is in agreement with the corresponding experimental one, with an error percentage of less than 2%. Similarly, the calculated peak due to the C—N modes of the ligand appears at 1275 cm^{-1}, falling within the experimental range. The experimental absorption spectrum of the ligand L_1(Fig. S7) shows two bands at 265–270 nm, which may be attributed to the $\pi \rightarrow \pi^*$ and $n \rightarrow \pi^*$ transitions. The absorption spectrum of the copper complex (Fig. S8) also shows a peak at 445 nm (22,472 cm^{-1}) which may be attributed to the $^2B_{2g} \rightarrow {}^2B_{1g}$ transition for the square planar geometry of the copper complex [53]. The electronic data of L_1 and the copper complex are listed in Table S4.

The IR spectrum of the N-(pyridin-2-yl)formamidine ligand (L_2) (Fig. S9) shows characteristic peaks at 1239 and 1629 cm^{-1} which are assigned to the stretching vibration of the C—N and (C═N) bands, respectively. Upon coordination with the Co(II) ion, the C—N and C═N bands are shifted to higher frequencies at 1279 and 1641 cm^{-1}, respectively, indicating the involvement of these groups in coordination [51]. This coordination mode was also confirmed by the X-ray crystal structure. $[Co(L_1)_2(H_2O)_2](NO_3)_2$ also shows characteristic peaks at 536 and 434 cm^{-1} which are assigned to Co—O and Co—N, respectively [52]. The experimental and theoretical vibrational spectra of the cobalt complex (Figs. S9 and S10) are in good agreement, as shown in Table S3. The theoretical IR data fall within the experimental ranges with a relative error in the range −0.01–0.145 cm^{-1}. The electronic spectrum of the L_2

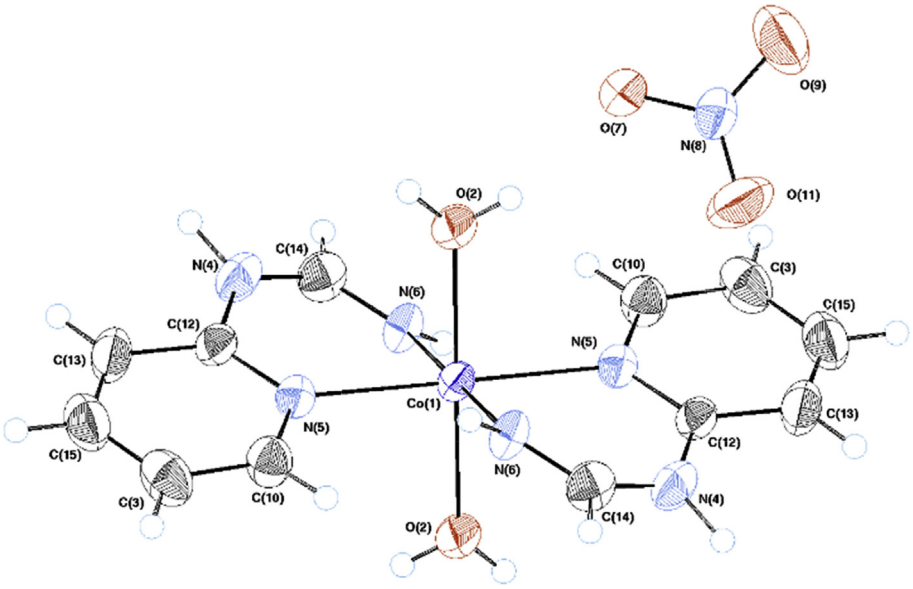

Fig. 3. ORTEP diagram of the $[Co(L_2)(H_2O)_2](NO_3)_2$ complex.

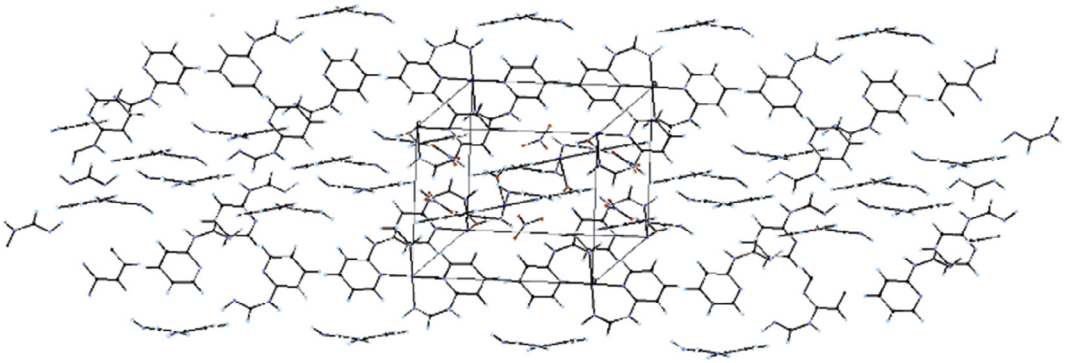

Fig. 4. Packing of $[Co(L_2)(H_2O)_2](NO_3)_2$.

ligand shows two bands at 270 and 315 nm (Fig S11) which may be attributed to the $\pi \rightarrow \pi^*$ and $n \rightarrow \pi^*$ transitions, respectively. The electronic data of the Co(II) complex are listed in Table S4. The spectrum of the Co(II) complex $[Co(L_2)_2(H_2O)_2](NO_3)_2$ shows two additional bands at 530 nm (18,868 cm^{-1}) and 505 nm (19,802 cm^{-1}) in the UV–Vis spectrum (Fig. S12) which are attributed to the $4T1g(F) \rightarrow 4A2g(F)$ and $4T1g(F) \rightarrow 4T1g(P)$ transitions, respectively, confirming the octahedral structure of the cobalt(II) complex [54].

3.2. Crystal structure description

All diagrams and calculations were performed using maXus (Bruker Nonius, Delft & MacScience, Japan) [55–59]. The crystal data and structure refinement are given in Table 1. The crystal structure of the Cu(II) complex consists of monomeric species (Figs. 1 and 2). The compound crystallizes in the space group $P2_1/c$, a = 8.5987(3) Å, b = 15.9778(6) Å, c = 10.6308(7) Å, V = 1321.07(11) $Å^3$, Z = 4, with the Cu(II) center having a distorted square planar structure. The ligand L_1 is coordinated to the Cu(II) center in a monodentate mode via the N4 atom. The chloride anion is also coordinated as a monodentate ligand. Selected bond length and angle data are collected in Table S1. The Cu—Cl (2.2766 Å) and Cu—N (1.964 Å) bond lengths are similar to those found in other Cu (II) complexes (reported values for Cu—Cl bonds ranged between 2.33 and 2.25 Å, while those for Cu—N bonds ranged between 1.98 and 2.01 Å) [53]. The values of the Cl—Cu—N bond angles ranged between 89.63 and 90.37°, showing small deviations from the ideal values for a square planar geometry, which may arise from the different sizes of the coordinated ligands.

The crystal structure of the Co(II) complex consists of monomeric species (Figs. 3 and 4). The compound crystallizes in the space group $P21/c$, a = 7.9187(2) Å, b = 10.8117(4) Å, c = 11.6687 (5) Å, V = 902.13(6) $Å^3$, Z = 4, with the Co(II) ion at the center of a distorted octahedral structure. The ligand L_2 is coordinated to the cobalt ion as bidentate via the N5 and N6 atoms, forming a 6-membered chelate, while water is coordinated as a monodentate ligand. Selected bond length and angle data are given in Table 2. The Co—O bond lengths (2.073 Å) are comparable with Co-O distances reported in the literature (2.067–2.122 Å) [60,61]. The Co—N bond length for the pyridine nitrogen atom of 2.121 Å is slightly longer than that of the imine nitrogen atoms (2.066 Å), whilst both of them are similar to those reported in the literature (2.142 Å for a Co—N pyridine bond and 1.976 Å for a Co—N imine bond) [62,63]. The single crystal X-ray diffraction study of the cobalt complex shows the existence of hydrogen bonding between the uncoordinated nitrate anion and the hydrogen atom of the coordinated water molecule, O(2)-H2A···O(11) and O(2)-H2B···O(7), with bond lengths of 2.047 and 1.990 Å respectively; such interactions help in packing the complex within the unit cell and

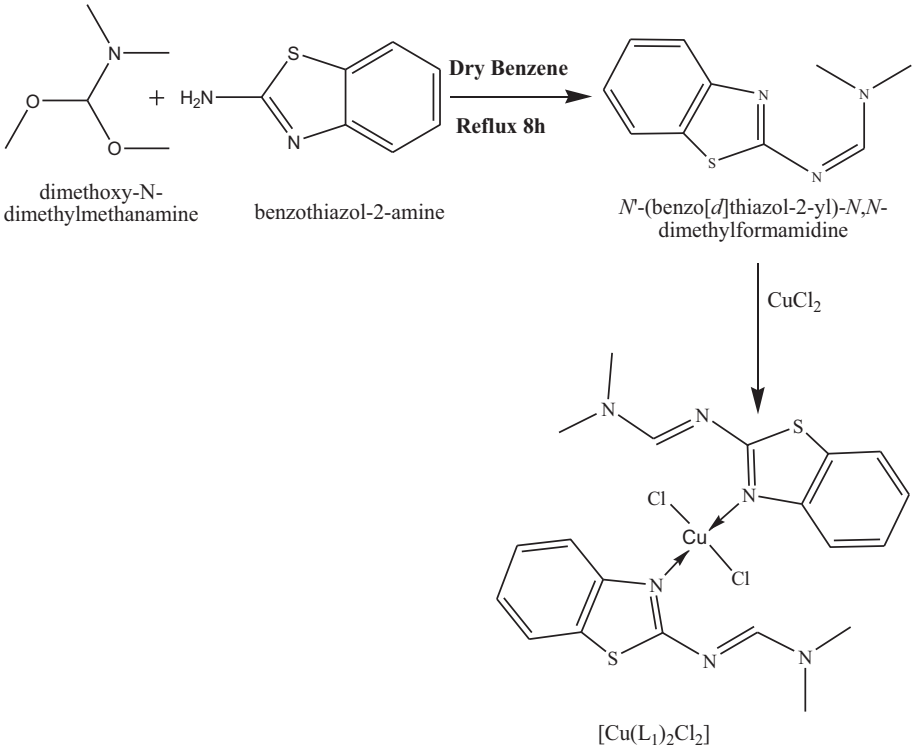

Scheme 2. Synthetic route to the[$Cu(L1)_2Cl_2$] complex.

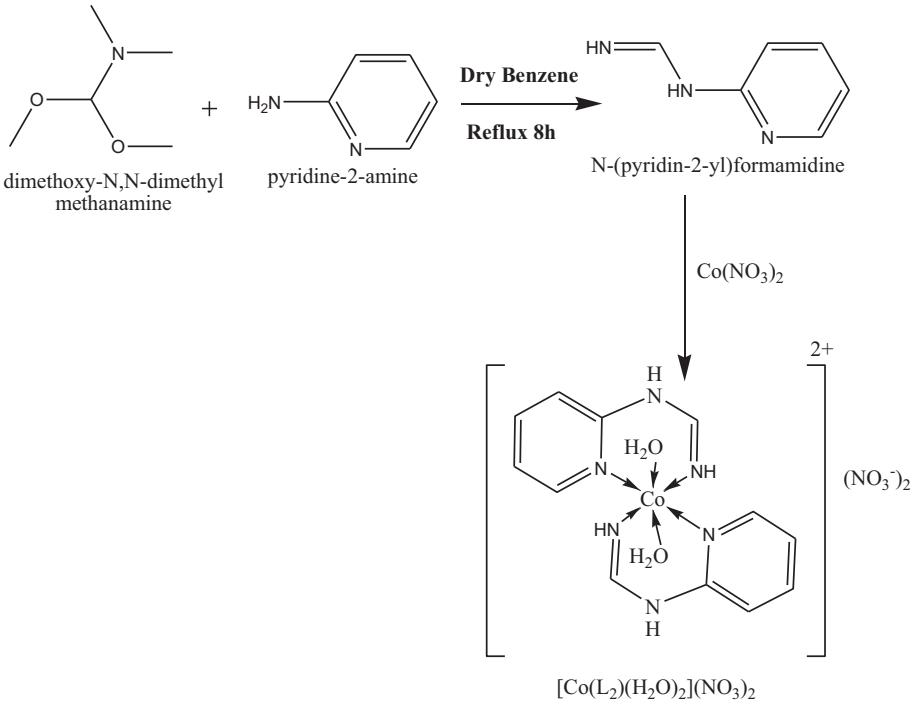

Scheme 3. Synthetic route to the $[Co(L_2)(H_2O)_2](NO_3)_2$ complex.

influences the space group; Table S5 [53]. This packing structure indicates that molecules of the cobalt complex are linked together via the O—H···O hydrogen bonds. The values of O2-Co-N5 range between 88.92 and 91.07°, showing small deviations from those of an ideal octahedral geometry.

3.3. Theoretical studies

The molecular structures of the singlet ground state of the complexes were carried out with DFT using the UB3LYP correlation functional [41,42], in addition to the 6-31G(d+) basis set [43,44],

Table 2
The calculated quantum chemical parameters of the ligands and their complexes.

$[Cu(L_1)_2Cl_2]$		$[Co(L_2)(H_2O)_2](NO_3)_2$	
$C_{10}H_{10}ClCuN_3S$	D_x = 1.525 Mg m^{-3}	$C_6H_9CoN_4O_4$	D_x = 1.915 Mg m^{-3}
M_r = 303.274	Mo Kα radiation	M_r = 260.095	Mo Kα radiation
Monoclinic	λ = 0.71073	Monoclinic	λ = 0.71073
$P2_1/c$	Cell parameters from 2664	$P2_1/c$	Cell parameters from 2029
a = 8.5987(3) Å	θ = 2.910–27.485°	a = 7.9187(2) Å	θ = 2.910–27.485°
b = 15.9778(6) Å	μ = 1.99 mm^{-1}	b = 10.8117(4) Å	μ = 1.90 mm^{-1}
c = 10.6308(7) Å	T = 298 K	c = 11.6687(5) Å	T = 298 K
α = 90.00°	Prismatic	α = 90.00°	Prismatic
β = 12. (18) × 10^{1}°	Dark green	β = 12. (18)x 10^{1}°	Orange
γ = 90.00°	Crystal source: Local laboratory	γ = 90.00°	Crystal source: Local laboratory
V = 1321.07(11) Å^3	Refinement on F^2	V = 902.13(6) Å^3	Refinement
Z = 4	Full matrix least squares refinement	Z = 4	Refinement on F^2
Data collection		Data collection	Full matrix least squares refinement
Absorption correction: none	R(all) = 0.099	Absorption correction: none	
5221 measured reflections	R(gt) = 0.050	3756 measured reflections	R(all) = 0.061
3358 independent reflections	wR(ref) = 0.101	2166 independent reflections	R(gt) = 0.046
1799 observed reflections	wR(all) = 0.111	1643 observed reflections	wR(ref) = 0.093
Criterion: I > 3.00 sigma(I)	wR(gt) = 0.101	Criterion: I > 3.00 sigma(I)	wR(all) = 0.095
R_{int} = 0.026	S(ref) = 1.888	R_{int} = 0.021	wR(gt) = 0.093
θ_{max} = 27.48°	S(all) = 1.857	θ_{max} = 27.51°	S(ref) = 1.492
h = −11 → 11	S(gt) = 1.893	h = −10 → 10	S(all) = 1.440
k = −20 → 18	1797 reflections	k = −12 → 14	S(gt) = 1.492
l = −13 → 13	160 parameters	l = −15 → 15	1641 reflections
h = 0 → 11	0 restraints	h = 0 → 10	133 parameters
k = 0 → 20	Only coordinates of H atoms	k = 0 → 14	0 restraints
l = −13 → 12	refined	l = −15 → 13	Only coordinates of H atoms refined

using Gaussian 09 (Institutional copy of the Faculty of Science, Cairo University) [45] in the gas phase and the output files were viewed by the GaussView 05 program. The optimized geometries of the ligands and complexes are given in Figs. S1–S4. Different quantum parameters were calculated to focus on the stability of the prepared complexes compared to those of the prepared ligands. TD-DFT (time-dependent density functional linear response theory) calculations were made to investigate the UV–Vis spectra of the complexes. Frequency calculations were performed using the optimized structures. The absence of negative frequencies confirms the full optimization of the complexes. The optimization data were in good agreement with the values of experimental X-ray data. Selected bond lengths and angles, compared to the experimental ones, are listed in Tables S1 and S2. The differences between the experimental and theoretical values are expected as the calculations were made in the gas phase. In the copper complex, the Cu-Cl bond length was 2.3257 Å, which is larger than the Cu—N bond length (2.033 Å), due to the large atomic radius of the Cl atom compared to that of the N atom. The bond angles surrounding the Cu(II) ion, ranging between 89.38 and 90.61°, indicate a slight distortion in the square planar geometry. Such a distortion may be due to the bulky formamidine ligands [35–37]. The bond angles between the Co(II) ion and the surrounding atoms of the water and formamidine ligands, varying from 87.55° to 92.45°, and the dihedral angles (179.98°) are deviated from those of a perfect octahedron (90°, 180°), indicating distorted octahedral structures. The determination of the atomic charges was used to study the electronic properties of the molecular systems. In the Cu(II) complex, there are three nitrogen atoms in the L_1 ligand with charge densities ranging from −0.429 to −0.644 (Fig S1). It was observed that the electron density on the coordinated nitrogen atom N4 increased after coordination due to MLCT – charge transfer from the copper ion to the π^* orbitals of the ligand. It is worth noting that the Cu(II) ion is coordinated to the nitrogen atom rather than the sulfur atom in this mode of coordination due to the fact that the sulfur atom possesses a positive charge, unlike the nitrogen atom which has a negative charge localized on it.

In the cobalt complex, there are three nitrogen atoms in the L_2 ligand with charge densities ranging between −0.690 and −0.500 (Fig S2). The Co(II) ion is coordinated to two nitrogen atoms (the nitrogen atom of a pyridyl group and the terminal nitrogen atom) in order to form a stable six membered ring including the cobalt ion; X-ray data confirm this suggested geometry. The electronic spectra of the ligands and the complexes were simulated in a vacuum environment. The excitation energies along with oscillator strengths for the complexes have been computed using the TD-DFT/6-31G*(d)/(U)B3LYP level of theory, with the calculations at the doublet level (S = 1/2) for the two complexes. The values for the excitation energies and oscillator strengths, along with the major transitions, are tabulated in Table S4. The energy diagrams of the complexes are shown in Figs. 5 and 6. The simulated and experimental electronic spectra of the complexes and ligands are shown in Figs. S7, S8, S11 and S12. The ligand L_1 showed peaks in DMF at 320 and 275 nm, while the ligand L_2 showed peaks at 315 and 270 nm. These energy bands are assigned to a mixture of ILCT (n -> π^* and π -> π^*), Table S4. In the copper complex, three low intensity peaks are obtained at 535 (MLCT), 445 (d-d transition) and 395 nm (LMCT), along with sharp bands at 290–360 nm (ILCT). In the cobalt complex, three low intensity peaks are obtained at 530 (d–d transition) and 505 nm (MLCT), along with sharp bands at 275–335 nm (ILCT).

The quantum chemical parameters of the formamidine ligands and complexes have been studied (Table 2). The calculated parameters include E_{HOMO}, E_{LUMO}, the energy gap (ΔE), absolute electronegativitiy (χ), chemical potentials (Pi), absolute hardness (η), absolute softness (σ), global electrophilicity (ω), global softness (S) and additional electronic charge (ΔN_{max}) [61–66]. In a complexation reaction, the metal usually acts as a Lewis acid (electron acceptor) and the ligand behaves like a Lewis base (electron donor). It is noted that the L_1 ligand possess a good softness σ value for coordinating the copper ion efficiently [67], the chemical potential Pi value also supports this suggestion. The frontiers molecular orbitals (HOMO and LUMO) determine the method of interaction for a compound with other species and they are key for studying the chemical reactivity of ligands and complexes.

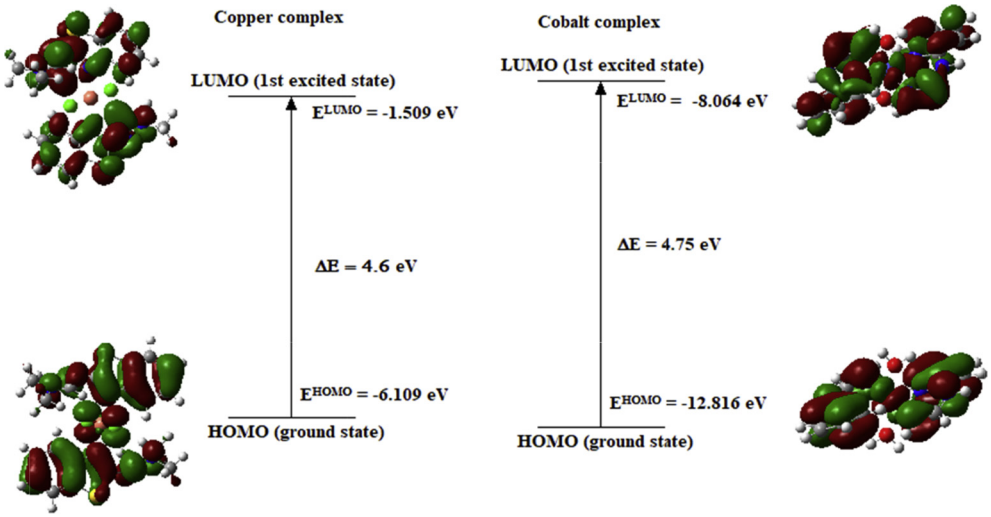

Fig. 5. HOMO–LUMO diagrams of the two complexes.

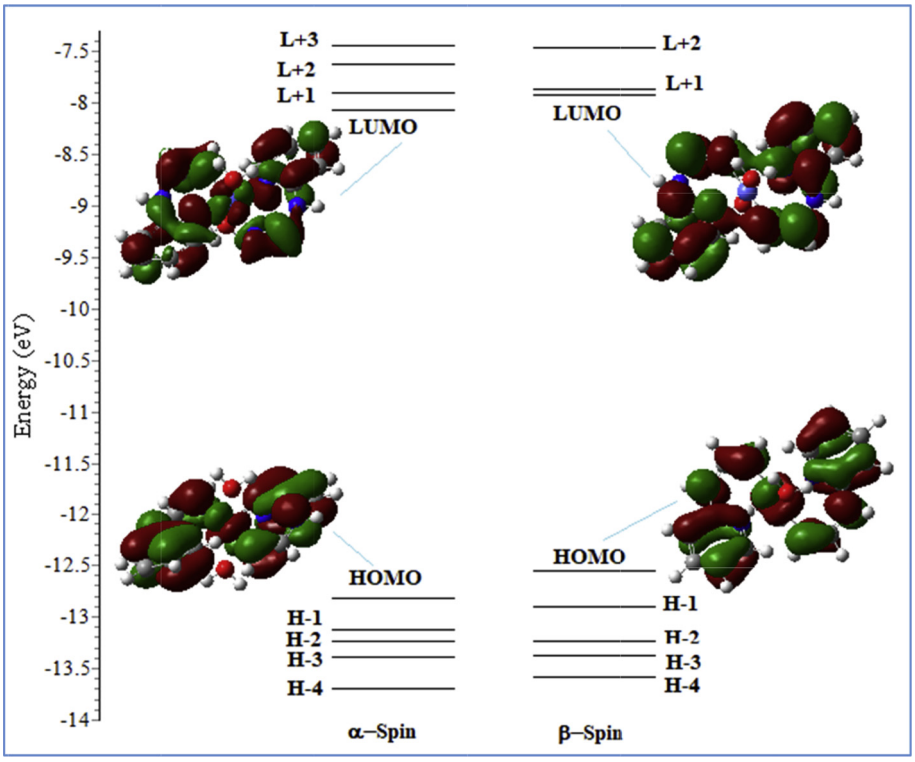

Fig. 6. The energy (eV), character and some contours of the molecular orbitals of the $[Cu(L_1)_2Cl_2]$ complex.

Negative charges of both the HOMO and LUMO energy levels suggest the stability of both the ligand and complex [68]. The HOMO–LUMO diagrams of the copper and cobalt complexes are shown in Fig. 7 and the energy gaps are equal to 4.60 and 4.75 eV, respectively; these energy gaps indicate that the two complexes are stable transition metal complexese [69].

Natural Bond Orbital (NBO) calculations [70] were performed at the B3LYP/6-31G(d+) level of theory. According to the NBO analysis for the copper complex, the electronic configuration of the Cu atom is: [core] $4s^{0.41}$ $3d^{9.42}$ $4p^{0.45}$ $4d^{0.01}$ $5p^{0.02}$, 18 core electrons, 10.27 valence electrons and 0.0334 Rydberg electrons, which gives a total of 28.26 electrons and a +0.688 charge on the Cu atom. From the NBO analysis for the cobalt complex the electronic configuration of the Co atom is: [core]$4s^{0.26}$ $3d^{7.63}$ $4p^{0.40}$ $4d^{0.05}$, 18 core electrons, 8.29 valence electrons and 0.0524 Rydberg electrons, which gives a total of 43.84 electrons and a +0.661 charge on the Co atom. The occupancies of the Co 3d orbitals are: d_{xy} 0.953, d_{xz} 0.977, d_{yz} 0.862, d^2_{xy} 0.518 and d^2_z 0.966. The formal charges on the donor atoms show that the electron distribution is not limited to the coordination bonds as the values of the computed formal charges of Cu (0.688 a.u.) and Co (0.661 a.u.) are smaller than +2. Such a decline in the charge value is expected upon complexation, with charge transfer from the metal centers to the ligands (MLCT) [70]. The molecular electrostatic potentials (MEPs) were used to show the electrophilic and nucleophilic moieties of the ligand. In the MEPs, the more reddish regions are regions with more negative parts of

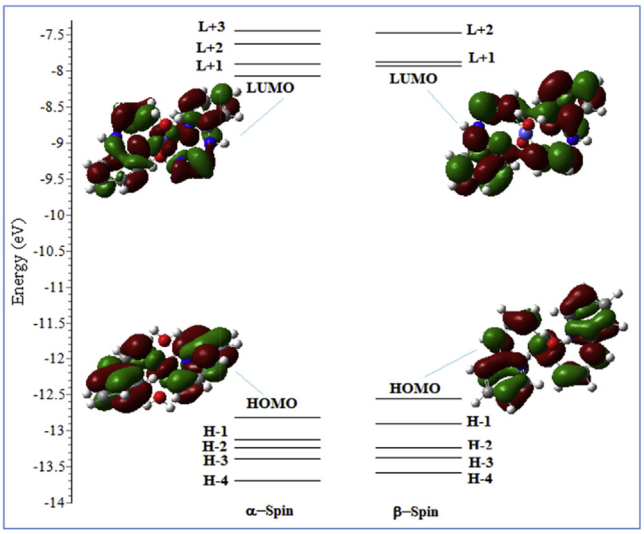

Fig. 7. The energy (eV), character and some contours of the molecular orbitals of the $[Co(L_2)(H_2O)_2](NO_3)_2$ complex.

the compound. The MEPs explain why the coordination of the ligands to the metals ions happen in this way (Figs. S15–S17). In the case of the L_2 ligand, the electron density is between the two nitrogen atoms. The cobalt ion is chelated to the ligands through these two nitrogen atoms because of the fact that the region between the two nitrogen atoms is more negative than any other regions in the ligand. In the L_1 ligand, the more negative region (reddish) is on the nitrogen atom N4 and that explains the reason why the copper ion is coordinated to it.

3.4. Evaluation of the antitumor activity using a viability assay

The cytotoxic activities of the ligands and complexes were investigated in vitro against human breast adenocarcinoma (MCF-7), liver carcinoma (HEPG-2) and colon carcinoma (HTC-116) cell lines. The IC50 value, defined as the drug concentration causing a 50% reduction in cellular viability, was calculated for each ligand and complex. The IC_{50} values (μg) of the tested ligands and complexes were compared with doxorubicin as a standard and the results are shown in Table 3 [35]. The cobalt complex showed higher IC50 values (less cytotoxicity) compared to the L_1 ligand for all the cell lines, and this may be attributed to the fact that the complex is charged and not neutral, thus there is a difficulty for passive diffusion into the cells. In contrast, the trans-copper complex showed lower IC_{50} values compared to the L_2 ligand; this is may be due to its neutrality and the presence of the chloride anion as a leaving group. Many trans-complexes of platinum [71,72], titanium [73] and copper [74] showed cytotoxic activity by different binding mechanisms than *cis*-platin. Preclinical studies in both murine and human tumor cell lines have identified the biochemical mechanisms affecting acquired resistance and cytotoxicity [72].

Table 3
IC_{50} values of the formamidine ligands and the metal complexes.

IC50 μg/well (μmole/well)			
	MCF-7	HCT-116	HepG-2
L1	5.09 (0.012)	5.23 (0.012)	8.32 (0.019)
L2	1.35 (0.003)	1.47 (0.005)	0.83 (0.002)
$[Cu(L_1)_2Cl_2]$	1.12 (0.0020)	2.66 (0.0048)	0.78 (0.0014)
$[Co(L_2)(H_2O)_2](NO_3)_2$	21.9 (0.047)	23.8 (0.051)	20.4 (0.044)
Ref. (Doxorubicin)	0.44 (0.0008)	0.47 (0.0008)	0.467 (0.0008)

These may be grouped into three broad classes, (a) differential uptake and/or efflux, (b) modulation of the platinum-DNA interaction, with subsequent effects on either the synthesis of DNA or repair capacity for the platinum-DNA lesions, and (c) enhanced sequestering of platinum by intracellular thiols, such as GSH and metallothionein.

4. Conclusion

Two new formamidine ligands and their homoleptic copper and cobalt complexes were prepared. The geometries of the complexes were confirmed using X-ray diffraction. Both the ligands and the complexes showed cytotoxic activity and the copper complex was more active compared to the ligand. The electronic structures and spectral properties of the ligands and the complexes have been explained by DFT and TD-DFT calculations.

Appendix A. Supplementary data

CCDC 1867161 and 1867162 contains the supplementary crystallographic data for $[Co(L_2)_2(H_2O)_2](NO_3)_2$ and $[Cu(L_1)_2Cl_2]$. These data can be obtained free of charge via http://www.ccdc.cam.ac.uk/conts/retrieving.html, or from the Cambridge Crystallographic Data Centre, 12 Union Road, Cambridge CB2 1EZ, UK; fax: (+44) 1223-336-033; or e-mail: deposit@ccdc.cam.ac.uk. Supplementary data to this article can be found online at https://doi.org/10.1016/j.poly.2018.12.020.

References

[1] E. Fujita, B.S. Brunschwig, T. Ogata, S. Yanagida, Coord. Chem. Rev. 132 (1994) 195.
[2] E. Kimura, S. Wada, M. Shiyonoya, Y. Okazaki, Inorg. Chem. 33 (1994) 770.
[3] B. De Clercq, F. Verpoort, Macromolecules 35 (2002) 8943.
[4] T. Opstal, F. Verpoort, Angew. Chem., Int. Ed. 42 (2003) 2876.
[5] B. De Clercq, F. Lefebvre, F. Verpoort, Appl. Catal. A 247 (2003) 345.
[6] S.L. Lambert, C.L. Spiro, R.R. Gagne, D.N. Hendriekson, Inorg. Chem. 21 (1982) 68.
[7] S. Brooker, Coord. Chem. Rev. 222 (2001) 33.
[8] V. Amendola, L. Fabbrizzi, C. Mangano, P. Pallavicini, A. Poggi, A. Taglietti, Coord. Chem. Rev. 219 (2001) 821.
[9] P.A. Vigato, S. Tamburini, Coord. Chem. Rev. 248 (2004) 1717.
[10] B. Woodard, R.D. Willett, S. Haddad, B. Twamley, C.J. Gomez-Garcia, E. Coronado, Inorg. Chem. 43 (2004) 1822.
[11] K. Ghosh, S. Pattanayak, A. Chakravorty, Organometallics 17 (1998) 1956.
[12] B. Rosenberg, L. Van Camp, J.E. Trosko, V.H. Mansour, Nature 222 (1969) 385.
[13] M. Gordon, S. Hollander, J. Med. (1993) 209.
[14] M. Gielen, E.R.T. Tiekink (Eds.), Metallotherapeutic Drugs and Metal-based Diagnostic Agents: The Use of Metals in Medicine, Wiley, 2005.
[15] K.D. Karlin, Z. Tyeklar, Bioinorganic Chemistry of Copper, Chapman & Hall, New York, 1993.
[16] C. Lin, J.D. Protasiewicz, T. Ren, Inorg. Chem. 35 (1996) 7455.
[17] C. Lin, J.D. Protasiewicz, E.T. Smith, T. Ren, Inorg. Chem. 35 (1996) 6422.
[18] T. Ren, C. Lin, P. Amalberti, D. Macikenas, J.D. Protasiewicz, J.C. Baum, T.L. Gibson, Inorg. Chem. Commun. 1 (1998) 23.
[19] M.H. Chisholm, F.A. Cotton, L.M. Daniels, K. Folting, J.C. Huffman, S.S. Iyer, C. Lin, A.M. Macintosh, C.A. Murillo, J. Chem. Soc., Dalton Trans. (1999) 13872.
[20] R. Clerac, F.A. Cotton, K.R. Dunbar, C.A. Murillo, X. Wang, Inorg. Chem. 40 (2001) 420.
[21] H. Lopez-Sandoval, M.E. Londono-Lemos, R. Garza-Velasco, I. PoblanoMelendez, P. Granada-Macias, I. Gracia-Mora, N. Barba-Behrens, J. Inorg. Biochem. 102 (2008) 1267.
[22] S. Akchaa, S. Gómez-Ruizb, S. Kellou-Tairic, L. Lezamad, F.B. Péreze, O. Benali-Baitich, Inorg. Chim. Acta 482 (2018) 738.
[23] L.M. Manus, R.J. Holbrook, T.A. Atesin, M.C. Heffern, A.S. Harney, A.L. Eckermann, T.J. Meade, Inorg. Chem. 52 (2013) 1069.
[24] T.A. de Toledo, P.S. Pizani, L.E. da Silva, A.M.R. Teixeira, P.T.C. Freire, J. Mol. Struct. 1097 (2015) 106.
[25] C. Balakrishnan, L. Subha, M.A. Neelakantan, S.S. Mariappan, Spectrochim. Acta Part A Mol. Biomol. Spectrosc. 150 (2015) 671.
[26] P. van der Gryp, S. Marx, H.C.M. Vosloo, J. Mol. Catal. A Chem. 355 (2012) 85.
[27] K. Sayin, D. Karakas, J. Mol. Struct. 1076 (2014) 244.
[28] I.F. Scheiber, J.F. Mercer, R. Dringen, Metabolism and functions of copper in brain, Prog. Neurobiol. 116 (2014) 33.
[29] R. Loganathan, S. Ramakrishnan, E. Suresh, M. Palaniandavar, A. Riyasdeen, M. A. Akbarsha, Dalton Trans. 43 (16) (2014) 6177.

[30] N.M. Urquiza, M.S. Islas, S.T. Ariza, N. Jori, J.J. Medina, M.J. Lavecchia, L.L. Tevez, L. Lezama, T. Rojo, P.A. Williams, E.G. Ferrer, Chem. Biol. Interact. 229 (2015) 64.
[31] S.M. Emam, I.E. El Sayed, N. Nassar, Spectrochim. Acta Mol. Biomol. Spectrosc. 138 (2015) 942.
[32] C. Rajarajeswari, M. Ganeshpandian, M. Palaniandavar, A. Riyasdeen, M.A. Akbarsha, J. Inorg. Biochem. 140 (2014) 255.
[33] S. Sobhani, M. Pordel, S.A. Beyramabadi, J. Mol. Struct. 1175 (2019) 677.
[34] J. Lu, H.-T. Liu, D.-Q. Wang, X.-X. Zhang, D.-C.h. Li, J.-M. Dou, J. Mol. Struct. 938 (2009) 299.
[35] M. Kabešova, R. Boca, M. Melnik, D. Valigura, M. Dunaj-Jurco, Coord. Chem. Rev. 140 (1995) 115.
[36] M. Du, Ch.-Peng Li, X.-J. Zhao, CrystEngComm 8 (2006) 552.
[37] B. Machura, A. Świtlicka, M. Penkala, Polyhedron 45 (2012) 221.
[38] A.A. Soliman, O.I. Alajrawy, F.A. Attabi, W. Linert, New J. Chem. 40 (2016) 8342.
[39] A.A. Soliman, O.I. Alajrawy, F.A. Attabi, W. Linert, Spectrochim. Acta A 152 (2016) 358.
[40] A.A. Soliman, O.I. Alajrawy, F.A. Attabi, M.R. Shaaban, W. Linert, J. Mol. Struct. 1115 (2016) 17.
[41] KAPPA-CCD software, Nonius B.V., Delft, The Netherlands, 1998.
[42] International Table for Crystallography, vol. C, Kluwer Academic, Dordrecht, the Netherlands, 1995.
[43] C. K. Johnson, ORTEP II. Report ORNL-5138, Oak Ridge National Laboratory, Oak Ridge, TN, 1979.
[44] A.D. Becke, J. Chem. Phys. 98 (1993) 5648.
[45] C. Lee, W. Yang, R.G. Parr, Phys. Rev. B 37 (1988) 785.
[46] G.A. Petersson, A. Bennett, T.G. Tensfeldt, M.A. Al-Laham, W.A. Shirley, J. Mantzaris, J. Chem. Phys. 89 (1988) 2193.
[47] G.A. Petersson, M.A. Al-Laham, J. Chem. Phys. 94 (1991) 6081.
[48] Gaussian 09, Revision C.01, M. J. Frisch, G. W. Trucks, H. B. Schlegel, G. E. Scuseria, M. A. Robb, J. R. Cheeseman, G. Scalmani, V. Barone, B. Mennucci, G. A. Petersson, H. Nakatsuji, M. Caricato, X. Li, H. P. Hratchian, A. F. Izmaylov, J. Bloino, G. Zheng, J. L. Sonnenberg, M. Hada, M. Ehara, K. Toyota, R. Fukuda, J. Hasegawa, M. Ishida, T. Nakajima, Y. Honda, O. Kitao, H. Nakai, T. Vreven, J. A. Montgomery, Jr., J. E. Peralta, F. Ogliaro, M. Bearpark, J. J. Heyd, E. Brothers, K. N. Kudin, V. N. Staroverov, T. Keith, R. Kobayashi, J. Normand, K. Raghavachari, A. Rendell, J. C. Burant, S. S. Iyengar, J. Tomasi, M. Cossi, N. Rega, J. M. Millam, M. Klene, J. E. Knox, J. B. Cross, V. Bakken, C. Adamo, J. Jaramillo, R. Gomperts, R. E. Stratmann, O. Yazyev, A. J. Austin, R. Cammi, C. Pomelli, J. W. Ochterski, R. L. Martin, K. Morokuma, V. G. Zakrzewski, G. A. Voth, P. Salvador, J. J. Dannenberg, S. Dapprich, A. D. Daniels, O. Farkas, J. B. Foresman, J. V. Ortiz, J. Cioslowski, D. J. Fox, Gaussian, Inc., Wallingford CT, 2010.
[49] T. Mosmann, J. Immunol. Methods 65 (1-2) (1983) 55.
[50] A.M. Sayed, (M.Sc. Thesis), Faculty of Science, Cairo University, 2013.
[51] A.A. Soliman, O.I. Alajrawy, F.A. Attabi, M.R. Shaaban, W. Linert, Spectrochim. Acta 152A (2016) 358.
[52] K. Nakamoto, Infrared and Raman Spectra of Inorganic and Coordination Compounds, fourth ed., Wiley, New York, 1986, p. 206.
[53] A.B.P. Lever, Inorganic Electronic Spectroscopy, second ed., Elsevier, Amsterdam, 1984, p. 544.
[54] B.S. Kusmariya, A. Tiwari, A.P. Mishra, G.A. Naikoo, J. Mol. Struct. 1119 (2016) 115.
[55] S. Mackay, C.J. Gilmore, C. Edwards, N. Stewart, K. Shankland, maXus Computer Program for the Solution and Refinement of Crystal Structures, Bruker Nonius, the Netherlands, MacScience, Japan & the University of Glasgow, 1999.
[56] C.K. Johnson, ORTEP–II. A Fortran Thermal–Ellipsoid Plot Program. Report ORNL-5138 (1976).
[57] Z. Otwinowski, W. Minor, 1997, in: Methods in Enzymology, 276, C. W. Carter, Jr. & R. M. Sweet (eds.), Academic Press, New York, pp. 307–326.
[58] A. Altomare, G. Cascarano, C. Giacovazzo, A. Guagliardi, M.C. Burla, G. Polidori, M. Camalli, J. Appl. Cryst. 27 (1994) 435.
[59] D. Waasmaier, A. Kirfel, Acta Cryst. A51 (1995) 416.
[60] K.E. Halvorson, C. Patterson, R.D. Willett, Acta Crystallogr. Sect. B B46 (4) (1990) 508.
[61] X.-M. Zhang, H.-S. Wu, X.-M. Chen, Eur. J. Inorg. Chem. (2003) 2959.
[62] E.J. Jung, U.K. Lee, B.K. Koo, Inorg. Chim. Acta 361 (2008) 2962.
[63] M. Masoudi, M. Behzad, A. Arab, A. Tarahhomi, H. Amiri Rudbari, G. Bruno, J. Mol. Struct. 1122 (2016) 123.
[64] R.G. Parr, R.G. Pearson, J Am Chem Soc 105 (1983) 7512.
[65] P. Geerlings, F. De Proft, W. Langenaeker, Chem Rev 103 (2003) 1793.
[66] R.G. Parr, Lv Szentpály, S, Liu, J Am Chem Soc 121 (1999) 1922.
[67] P.K. Chattaraj, S. Giri, J Phys Chem A 111 (2007) 11116.
[68] G. Speier, J. Csihony, A.M. Whalen, C.G. Pie-pont, Inorg Chem 35 (1996) 3519.
[69] S. Sagdinc, B. Koksoy, F. Kandemirli, S.H. Bayari, J Mol Struct 917 (2009) 63.
[70] A.M. Mansour, Inorg. Chim. Acta. 394 (2013) 436.
[71] S.M. Aris, N.P. Farrell, Eur. J. Inorg. Chem. (2009) 1293.
[72] N. Farteli, L.R. kt-Hand, J. Roberts, M. Van Beusichem, Cancer Research 52 (1992) 5065.
[73] A. Tzubery, E.Y. Tshuva, Inorg. Chem. 50 (2011) 7946.
[74] A.N. Kate, A.A. Kumbhar, A.A. Khan, P.V. Joshi, V.G. Puranik, Bioconjugate Chem. 25 (2014) 102.